Microstructure, Crystal structure and ionic conductivity of 3 mol % (Fe, Mn, Co, Zn) doped 8YSZ

Z.A. Ahmad[1], *B.* Johar[2,*], *S.* Tinesha[2], *S.F.* Khor[2] , and *E.K.* Kok[2]

[1]School of Materials Engineering, Universiti Sains Malaysia,
[2]School of Materials Engineering, Universiti Malaysia Perlis, 02600 Kangar, Perlis, Malaysia

Abstract. Effect of 3 mol% of transition elements doped 8YSZ such as YSZZn, YSZFe, YSZCo and YSZMn on the ionic conductivity. SOFCs mostly operate at higher temperature. By substitute with dopants, it can reduce the operating temperature and costs. In this experiment, 3 mol% dopants mixed with 8YSZ and sintered at 1550 °C, hold for two hours. Crystal structure, microstructure, sintering behaviour and ionic conductivity at 300 °C were investigated. XRD demonstrates three phases (cubic, monoclinic and tetragonal) were obtained. It was confirmed that small additions of TMOs (Mn, Fe, Co and Zn) promotes densification, grain growth and ionic conductivity compared to pure 8YSZ. YSZZn obtained the highest ionic conductivity, 3.55×10^{-3} mS cm^{-1} at 300 °C.

1 Introduction

Pure zirconia exists in three crystallographic phases such as low temperature monoclinic phase (space group P21/c), intermediate temperature tetragonal phase (space group P42/nmc) and high temperature cubic phase (space group Fm3m) [1]. Zirconia has a fluorite type of crystal structure. During cooling process, it is about 3-5% volume expansion will form due to the transformation from tetragonal to monoclinic phase, which limit usage of ZrO_2 ceramics as structural material [2]. Monoclinic phase and tetragonal phase is not stable enough. Hence, this unstable condition was overcome by adding stabilizing agents to maintain the structure [3]. Thus, cubic ZrO_2 is stable above 2300 °C or can be stabilized by cation substitution. This is supported by Basu et al. had found that direct substitute of small amount of divalent or trivalent cations at the host lattice (Zr^{4+}) has stabilized the zirconia phase. Impurities that were commonly used are Y_2O_3, Yb_2O_3, Sc_2O_3, Gd_2O_3, Dy_2O_3, Nd_2O_3, Sm_2O_3, CaO, MgO and others [4].

Yttria doped zirconia has been widely used in variety of industrial applications [5]. Yttria stabilized zirconia (YSZ) broadly applies as a typical solid ionic conductor such as electrolyte of solid oxide fuel cell (SOFC) [3] and it was established as an oxide ion conducting ceramic[6-8]. Properties of SOFC are low thermal conduction, high ionic conductivity and chemical stability in both oxidizing and reducing atmosphere[7, 9]. Dopants plays important role to enhance the chemical and mechanical properties on

---

* Corresponding author: banjuraizah@unimap.edu.my

ceramic body. It can affect on the grain boundaries conductivity (GB) and grain interior (GI) during sintering process. It has been confirmed that transition metal oxides are effective sintering promoters for densification of SOFC electrolytes. As reported by Zhang and Du et al.,doping of transition metal oxides (TMOs) such as Mn and Ni was found to be an effective sintering aids for zirconia ceramic [10]. Grain interior is the disintegration of dopant in the electrolyte lattice doping can increase or decrease on grain boundary conduction. Grain growth can affect the ionic conductivity and transformation of crystal structure.Meng and Miao et al. reported that incorporation of heterogeneous and homogeneous doping. In homogeneous doping, oxygen vacancies will replace the atoms at normal lattice sites of zirconia with different of dopants [3]. A high content of dopant (Ca^{2+}, Y^{3+} and others) concentration can cause a few deformities and consequently resulted in lower ionic conductivity. Therefore, homogeneous doping has its limit to improve the ionic conductivity of YSZ. On the other hand, heterogeneous doping is insoluble in host YSZ and remains physically distinct phase. It influences the ionic conductivity of YSZ according to the space charge hypothesis [3] .

Thus, type and quantity of dopants utilisation depends on the stability limit. Kawada et al. stated that 4 mol% of Mn doped is the maximum stability limit of zirconia. Besides, Dey and Das Sharma et al. had reported that stability limit of transition metals such as iron doped with 2 mol% can increase rapidly in the sinterability of powders [4]. Additionally, Shiratori et al. developed that full stabilization and maximum solubility can occur in MgO with values of 12.1 and 14.1 mol% respectively [11]. Phase diagram can identify the solubility limit of each component which occurs at what temperature. Doping transition metals such as Zn, Fe, Mn and Co were chosen added in 8YSZ due to its ionic radius smaller than yttria (0.9 Å). Ionic radiuses of Zn, Fe, Mn and Co are 0.74 Å, 0.645 Å, 0.46 Å and 0.745 Å respectively. Therefore, a main reason of this research is to investigate the 3 mol% transition metals (Fe, Co, Mn and Zn) doped with 8YSZ by focusing on the crystal structure, microstructure and ionic conductivity at 300 °C.

2 Methodology

2.1 Sample preparation

8YSZ (size range from 0.020 to 200 μm) powder were used as a main precursors ZrO_2 (<3.8% monoclinic phase, Sulzer Metro (US) Inc) and the elemental analysis of the powders is tabulated in Table 1. Dopants manufactured from HmbG Chemicals and Sigma. Dried mass of 3 mol% of dopant (MnO, FeO, CoO and ZnO) were mixed with 8YSZ powders ground with mortar pestle for 30 minutes. Calcinations process were performed at 1000 °C for 1 hour and mixed powder with 1.5g were press into pellets of 12mm diameter with 2mm thickness at 6 tonne pressure automatically by Automatic hydraulic press, model 3890.4NE000. The pellets were sinteredat 1550 °C in air hold for two hours with heating rate at 10°C/min.

Table 1 Elemental analysis of 8YSZ.

Chemical analysis	Value (WT %)
Al_2O_3	0.02
Fe_2O_3	0.02
HfO_2	1.7
MgO	0.03
SiO_2	0.2
TiO_2	0.05
Y_2O_3	7.6
ZrO_2	90.2
CaO	0.02
Organic Solids	0.1
Uranium + Thorium	0.02

2.2 Sample characterization

Thermal analysis of doped YSZ ceramic powders were carried out using DTA/TG machine model Perkin Elmer Thermoanalyser started at room temperature until 1600°C. DTA was used to observe all the decomposition reactions (heat absorption or liberation) and determine the crystallization behavior, while TGA was used to detect the loss in mass (degradation).X-ray diffraction (XRD) patterns of the primary powders and sintered specimens were respectively measured with XRD instrument powders at 40kV and 100mA using Cu Kα radiation in air at room temperature. The diffraction intensity was measured step wise every 0.02° in the diffraction angle 2θ range between 5° and 90°. Rietveld Refinement method using XpertHighScore Plus software was used to quantify phase and refine the crystal structure. The relative densities were measured by Archimedes method. After well polished, sintered pellet ceramics sample coated with platinum (pt) using sputter coater prior characterized using the SEM. Morphology of sintered pellets were observed on different magnifications 100X, 500X, 1000X and 10,000X at 15kV by model JEOL JSM-6460LA.The ionic conductivity of sintered doped 8YSZ ceramic samples were measured by using impedance analyser, model Agilent 4294A at 300 °C. The testing was conducted at frequency range from 5000,000 Hz to 4 Hz will be measured.

3 Results and discussion

3.1 Results of DTA/TG

The experiments are carried out by differential thermal (DTA) and thermogravimetric (TGA) analysis method using a Perkin Elmer Thermoanalyser instrument. The heat flow and weight change of calcinated powder samples placed in Al_2O_3 crucibles were measured from room temperature to 1600 °C at a heating rate of 10 °C per minute. Weight gain in TG curve as shown in Fig.1 may attributes to weight gain that attributed to the oxidation [12]. YSZ, YSZMn and YSZFe gain about 0.20 mg of weight at 1500 °C. Cobalt shows an increase of weight about 0.21 mg. However, weight of dopant zinc gain about 0.205 mg at 1300 °C and loss to 0.19 mg.

DTA curves can be seen in Figure 2and as shown in the figureallundopedand doped 8YSZ samples undergoes exothermic reaction at beginning of 200 °C. YSZ, YSZCo and YSZZn undergo two endothermic peaks at each curve, while YSZFe and YSZMn undergo only one endothermic peak. It can seen clearly in Fig. 2, first endothermic peaks in DTA curve for the YSZZn happens between range 500 °C to 600 °C undergo oxidation by the air

atmosphere. When temperature exceeds 550 °C and reach 600 °C, an endothermic reaction of YSZZn undergo having the maximal temperature shift at 565 °C. Simultaneously around 7% mass gain was detected. On the other hand, endothermic reaction of YSZ occurred at 600 °C. However, change in slope of YSZCo occurs at 936 °C could be due to the addition of Co^{2+} to Co^{3+} causing chemical expansion due to high temperature. In addition, YSZZn, YSZFe and YSZMn curves show a sudden change and broad endothermic reaction approximately from 1100 °C to 1250 °C. This change in the kind of thermal process is considered as occurrences of phase transformation, crystallization and structural distortion.
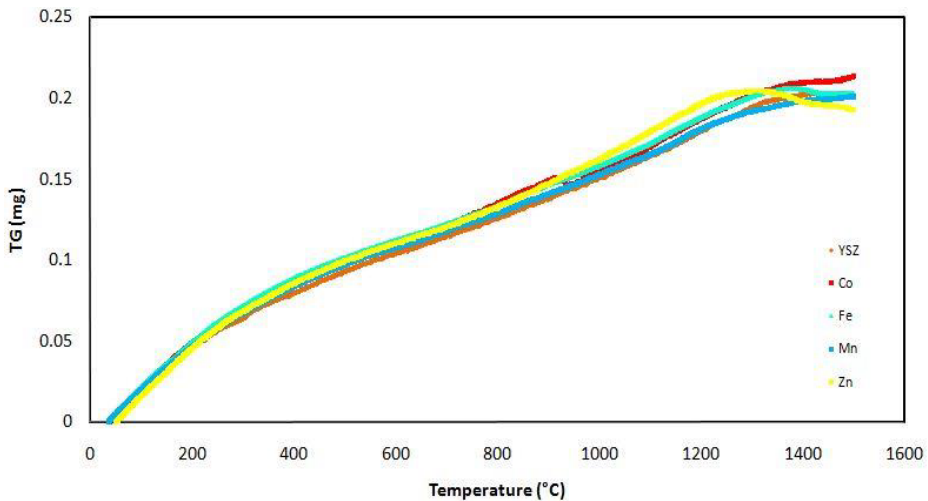

Fig. 1. TGA curve for the different transition metals doped 8YSZ. Dopants include Co, Fe, Mn and Zn.
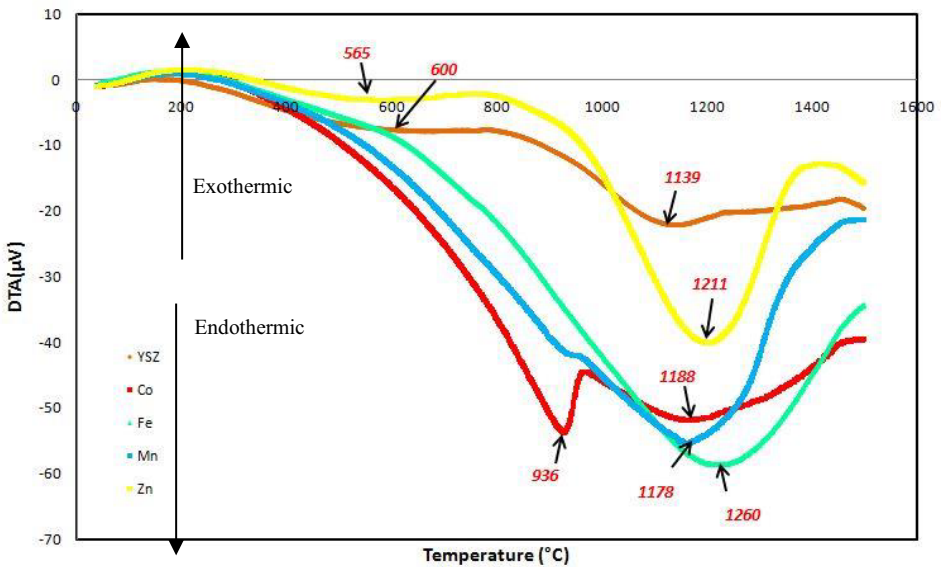

Fig. 2. DTA curve for different transition metals doped YSZ. Dopants include Co, Fe, Mn and Zn.

Two distinct features are observed from other sample: shifting in Bragg's diffraction towards higher 2θ which gives a decrease in lattice volume and appearances of shoulders in

the XRD patterns corresponding to the diffraction planes indicating lower crystal symmetry [13]. Previous research mentioned that distortion of the oxygen lattice results in the tetragonal symmetry in sintered YSZ [9]. The crystalline structure of pellets was analyzed by X-ray diffraction (XRD). Figure 3 shows the x-ray diffraction of the sintered pellet of YSZMn, YSZFe, YSZCo and YSZZn along with pure YSZ. For the doped powder (up to dopant concentration of 3 mol%), all peak corresponding to the YSZ (cubic/c, tetragonal/t and monoclinic/m) are observed.Cubic phase exhibits only single peak at all positions due to broadening of peak, Z polymorph might overlap, thus crystal structure refinement using whole profile fitting method or Rietveld method to determine present either one of both polymorph.
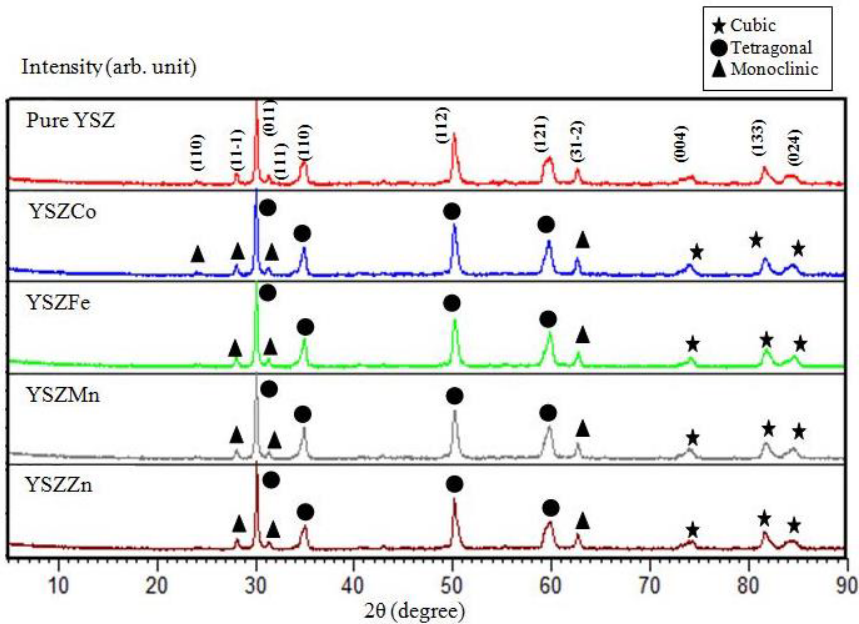

Fig. 3. Comparative XRD patterns of undoped 8YSZ and YSZCo, YSZFe, YSZMn and YSZZn.

Table 2. Refinement XRD result.

Element	Tetragonal	Cubic	Monoclinic	RWP
YSZ	65.5	26.8	7.8	13.66
YSZMn	82.4	12.4	5.2	13.25
YSZFe	77.5	17.7	4.8	13.73
YSZZn	78.9	16.1	5.0	12.80
YSZCo	80.2	14.3	5.5	13.43

    Table 3 demonstrates the density of all sintered samples using Archimedes. It shows relative density of sample increasing with dopant concentration of 3 mol %. Liquid phase promotes the diffusion rate of 8YSZ matrix, enhance densification and grain growth [14].

Table 3. Result of Archimedes.

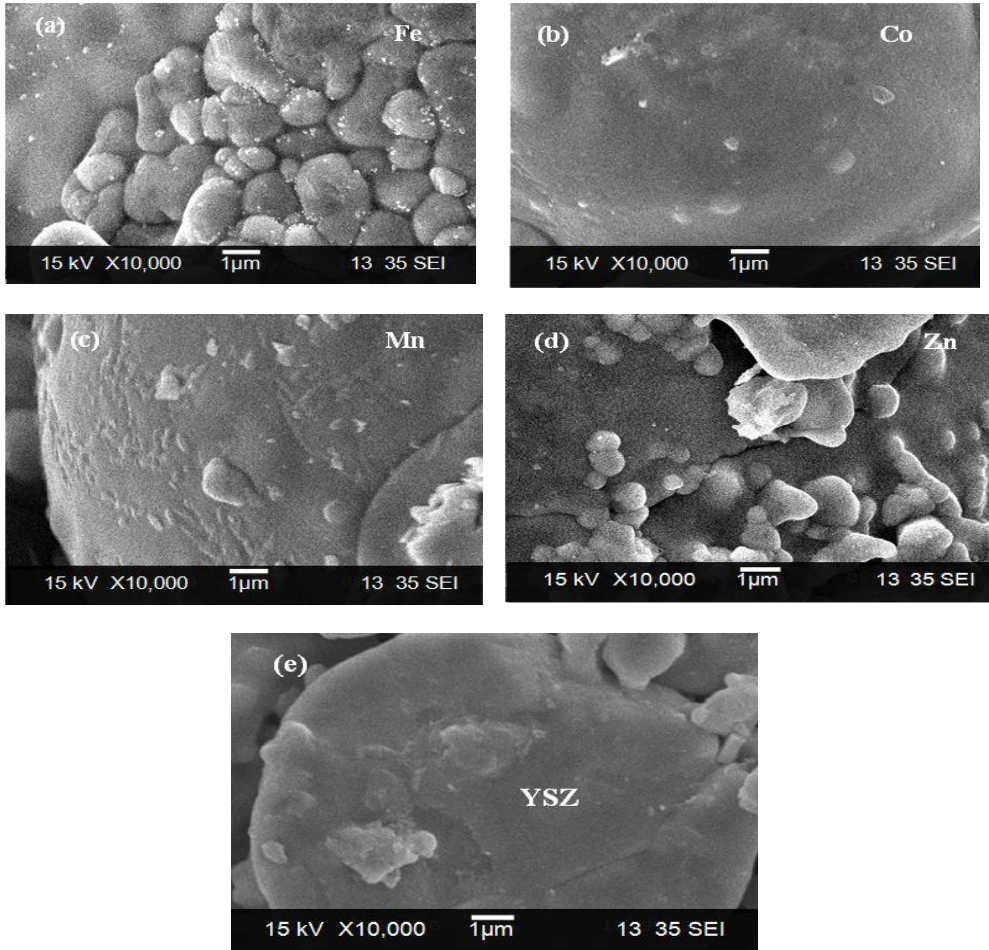| Composition	Dry mass (g)	Mass in water (g)	Bulk Density (kg/m^3)	Densification, %
Pure YSZ	1.14	0.94	5.539	75.85
3% Fe	1.49	1.22	5.143	74.13
3% Mn	1.46	1.19	5.420	83.25
3% Zn	1.47	1.19	5.306	76.32
3% Co	1.49	1.20	5.157	78.96

Fig. 4. The SEM micrographs showing the surface morphology of 3% of transition elements (a) YSZFe, (b) YSZCo, (c) YSZMn, (d) YSZZn and (e) undoped 8YSZ sintered at 1550 ^{o}C for 2h.

Figure 4 demonstrates the morphology of SEM images of the pellets of YSZCo, YSZMn, YSZFe and YSZZn after sintered at 1550 °C for 2h. Pure YSZ shows in Fig 4(e), YSZ in spherical shape which is similar to the microstructure previously reported by Pradhan [15, 16]. In Fig 4(a) and (d), YSZFe and YSZZn crystallite structure grows and agglomerates between the grain boundaries. In addition, YSZFe shows the least porosity and densification about 74%. Iron atoms easily trap vacancies within the grain boundary and started agglomerate along the grain boundaries. The sample of YSZCo and YSZMn

were not well sintered; the micrograph revealed some open pores, showing not fully densified microstructure, it lead to relative density values being less than 100% [14]. Hence, it can conclude that sinterability of specimen prolonging the holding time, whereas ionic conductivity may improve by increasing the density.

It proposed that cause of stability of tetragonal phase in studies directly related problem statement of raw powder (8YSZ). During heat treatment of the Y_2O_3 doping either diffuse into ZrO_2 crystal lattice or segregation at grain boundary, depend how yttria atom fuses with Zr atom during synthesis process. YSZMn shows the highest porosity about 25% at 1550 °C. Undoped 8YSZ was dense with small close pore, rapid densification of MnO added specimen may attributed of liquid phase sintering. Liquid phase promotes the diffusion rate of 8YSZ matrix, enhance densification and grain growth [14]. Previous research of Vijaya Lakshmi on stabilization effect on Mn is not well established in phase diagram. Shultz and Muan reported that maximum solubility of 27 mol% of MnO in ZrO_2 at 1673 K. Mn can present in trivalent state with ionic radius of 0.065nm to have any stabilization effect [17].

Conductivity depends on the difference between size of host and dopant cation radii. High conductivity in solid oxide is associated of oxygen vacancies and dopant cations into imperfections of low mobility. Generally, concentration of dopant and size of acceptors are important in ionic conductivity of stabilized zirconia. Kosacki and Rouleau et al. had mentioned that acceptor with an ionic radius nearly similar to Zr^{4+} ion, of which Y^{3+} due to minimum activation energy. The low frequency region is undergo DC, increase in conductivity at high frequency [18]. YSZZn has highest ionic conductivity and combination of DC and AC. YSZZn has DC value of conductivity about 5×10^{-3} Sm^{-1} until 100K Hz. Furthermore, YSZFe stated that it has DC value of conductivity about 3×10^{-5} $mScm^{-1}$ until 5K Hz. YSZCo, YSZMn and YSZ curves undergo weak DC contribution among the atoms. As a result, TMOs reduces the total conductivity of pure 8YSZ of 0.5×10^{-6} Sm^{-1}. Consequently, 3% mol of YSZFe can reduce the GI conduction by ~27-33% [4].

There are two semicircles for the impedance plots measured at 300 °C. The left semicircles results from the grain resistance, while the right one is due to grain boundary resistance. As the measurement temperature increases, the capacitance of the grain boundary and grain become comparable, leading disappearance of one semicircle corresponding to grain. Ionic size of TMOs are small compared with yttria, as a result of TMO dissolution still present at >1550 °C which associated oxygen vacancies should be freed. From the previous research, Wang et al. proposed that addition of ZnO gives an adverse reaction to the conductivities [19]. Besides that, Shujun et al. had investigated that highest ionic value of 1 mol% of Zn doped $Ce_{0.8}Y_{0.2}O_{1.9}$ was 0.0516 Scm^{-1} at 750 °C [14].
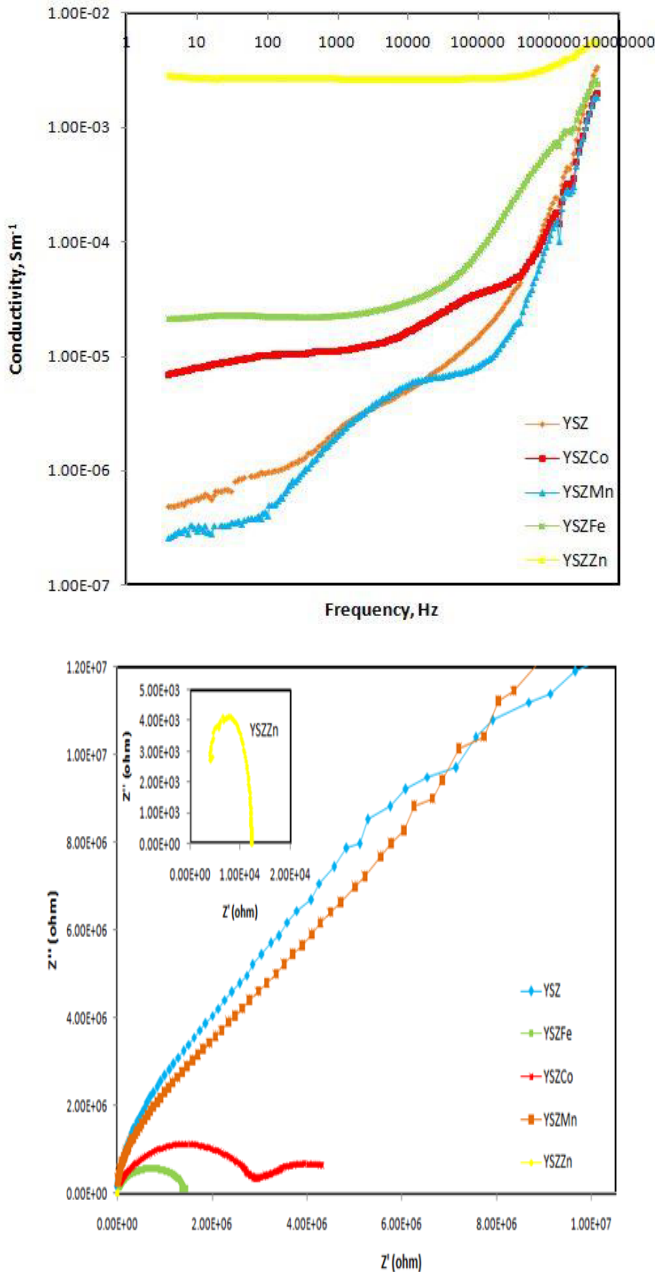
Fig. 5. Logarithmic relation between ionic conductivity (log σ) and frequency at 300 °C. Impedance diagrams recorded at 300 °C for different transition metals doped YSZ such as YSZCo, YSZFe, YSZMn and YSZZn.

In previous study, ZnO decrease the activation energy of conduction, hence it increase ionic conductivity [14]. 3 mol% ZnO of dopants can lead to increase in the sintered density value. Ionic conductivity of 3 mol% of YSZZn has highest ionic conductivity with 3.55 X 10^{-3} mS cm^{-1}. Besides that, value of conductivity of 3 mol% of cobat was 3.32 X 10^{-4} mS cm^{-1} was measured in air atmosphere. On the other hand, Fe_2O_3 cannot stabilize the cubic phase of ZrO_2 by its own. So, partial substitution of Fe^{3+} for Y^{3+} can increase the Y_2O_3

efficiency as a stabilizer of c-ZrO[20]. Ionic conductivity can be increase by the oxygen vacancies by the content of aliovalent substitution such as Fe^{3+} and Y^{3+}. Fe^{3+} ion migrate by a vacancy diffusion mechanism during sintering process. Fe^{3+} can either substitute or interstitial doped 8YSZ, this is due to the ionic radius of Fe^{3+} ions (0.55Å – 0.78Å) are far smaller than Zr^{4+} ions (0.84Å) and Y^{3+} ions (1.019Å) [7]. Furthermore, diffusion coefficient, D increases due to contribute of partially interstitial defect of Fe^{3+}. Thus, Fe^{3+} ion can weaken the bond strength of Zr-O bond. Greater activation energy is associated with a greater ionic radius. Presence of the weaken bond can led to decrease in activation energy, which partially contribute increase in the diffusion coefficient D. When temperature up to 300 °C, the value of conductivity of 3 mol% of iron is 2.67×10^{-3} mS cm^{-1} was measured in air atmosphere.

4 Conclusions

Themajor conclusion of the present work is to study the effect of dopants in electrolytes. YSZ solid solutions doped with small amounts of Zn, Mn, Fe and Co were investigated. It was found that the doping of 8YSZ with 3 mol% transition elements is found to be effective in lowering sintering temperature. From detailed of XRD analysis, no appreciable of new phase formation has been noticed up to 3mol%, dopants are completely dissolved in the 8YSZ. Hence, it could be that dopants mixed of metal oxides did not react with pure YSZ at 1550 °C. Pure YSZ and TMOs in this present study requires higher sintering temperature. Hence, it found that the corresponding electrochemical performances of YSZFe, YSZMn, YSZZn and YSZCo found performed better than fabricated by undoped YSZ. Based on their doping effect on grain growth and ionic conductivity, YSZZn can reduce porosity and improve sinterability to obtain dense electrolyte material.

References

1. Y. Zhou, W. Yuan, Q. Huang, W. Huang, H. Cheng, H. Liu, Ceram. Int., **41**, 10702 (2015)
2. B. Xie, C. He, P. Cai , Y. Xiong, Thin Solid Films, **518**, 1958 (2010)
3. B. Meng, Z.Y. Miao, M. Kong, X.X. Liu, J. Yu, Q.Q. Yang, Solid State Ionics, **258**, 61 (2014)
4. T. Dey, A.D. Sharma, A. Dutta, R.N. Basu, J. Alloy. Compd., **604**, 151 (2014)
5. A. Madani, A. Cheikh Amdouni, A. Touati, M. Labidi, H. Boussetta, C. Monty, Sensor Actuat. B-Chem., **109**, 107 (2015)
6. N. Matsui, M. Takigawa, Solid State Ionics, **40**, 926 (1990)
7. F. Guo, P. Xiao, J. Eur. Ceram. Soc., **32**, 4157 (2012)
8. S.K. Vijay, V. Chandramouli, S. Khan, P.C. Clinsha, S. Anthonysamy, Ceram. Int., **40**, 16689 (2014)
9. R.L. Gonzalez Romero, J.J. Melendez, D.G. Garcia, F.L. Cumbrera, A.D. Rodriguez, Solid State Ionics, **219**, 1 (2012)
10. T.S. Zhang, Z.H. Du, S. Li, L.B. Kong, X.C. Song, J. Lu, J. Ma, Solid State Ionics, **180**, 1311 (2009)
11. Y. Shiratori, F. Tietz, H.J. Penkalla, J.Q. He, Y. Shiratori, D. Stover, J. Power Sources, **148**, 32 (2005)
12. M. Jamshidijam, R.V. Mangalaraja, A. Akbari Fakhrabadi, S. Ananthakumar, S.H. Chan, Powder Technol., **253**, 304 (2014)
13. M.K. Mahapatra, N. Li, A. Verma, P. Singh, Solid State Ionics, **253**, 223 (2013)
14. S. Li, L. Ge, H. Gu, Y. Zheng, H. Chen, L. Guo, J. Alloy. Compd., **509**, 94 (2011)

15. M. Pradhan, P.C. Kapur, Pradip, Ceram. Int., **38**, 2835 (2012)
16. Z. Shu, X. Jiao, D. Chen, J. Alloy. Compd., **509**, 9200 (2011)
17. H. Misawa, K. Nakata, J. Matsuura, Y. Moriwaki, K. Kawashima, T. Shimizu, T. Shirasawa, R. Takahashi, Neurobiol. Dis., **23**, 169 (2006)
18. M. El Moudane, M. El Maniani, A. Sabbar, A. Ghanimi, M. Tabyaoui, A. Bellaouchou, A. Guenbour, Mater. Res. Bull., **72**, 241 (2015)
19. C.X. Wang, J.C. Lv, Y. Ren, T. Zhi, J.Y. Chen, Q.Q. Zhou, Z.Q. Lu, D.W. Gao, L.M. Jin, Appl. Surf. Sci., **359**, 196 (2015)
20. O. Bohnke, V. Gunes, K.V. Kravchyk, A.G. Belous, O.Z. Yanchevskii, O.I. V'Yunov, Solid State Ionics, **262**, 517 (2014)